

Structural Studies of Doped Lanthanum Orthoferrites of Interest for SOFCs

Isabella Natali Sora*, Valeria Felice, and Francesca Fontana

INSTM R.U. Bergamo and Università di Bergamo, Dipartimento di Ingegneria e Scienze Applicate, Viale Marconi 5, 24044 Dalmine, Italy
 isabella.natali-sora@unibg.it

Traditional LSM ($\text{La}_{1-x}\text{Sr}_x\text{MnO}_{3-w}$) SOFC cathode material shows some drawbacks operating below 800 °C, in particular poor oxygen ion conduction, which limits the active area of the electrode to the three phase boundary (TPB) between electrolyte, electrode and gas phase at the interface. A strategy to overcome this problem consists in the development of materials with both good oxygen ion and electronic conductivity, in which oxygen ions catalytically dissociated on the surface are able to reach the electrolyte by diffusion in the bulk of the cathode. $\text{La}_{1-x}\text{Sr}_x\text{FeO}_{3-w}$ has been proposed as possible SOFC cathode, in search for a high activity at lower temperatures with respect to LSM. The aim of the work is the structural study of alternative cathodic materials for intermediate temperature solid oxide fuel cells, mainly based on ABO_3 perovskite-type lanthanum ferrite. Within this framework the effects of A (La)-site doped with Sr or B (Fe)-site doped with Ta on the crystal structures of these materials were investigated by X-ray powder diffraction (XRPD). In conjunction with the experimental results, the microscopic mechanisms of the doping effect were discussed providing deeper understanding into structure-property relations.

1. Introduction

SOFCs (Solid Oxide Fuel Cells) are devices where H_2 or hydrocarbons and O_2 are electrochemically reacted to produce water, electricity and heat. Most of the materials proposed for SOFC are the traditional Ni-YSZ / YSZ / LSM assembly. In particular, the most used cathode material for SOFC is a perovskite oxide $\text{La}_{1-x}\text{Sr}_x\text{MnO}_3$ (LSM), which is a mixed ionic-electronic conductor successfully applied as cathode material in YSZ-based high-temperature HT-SOFCs; however it shows higher overpotential at intermediate operating temperatures (IT) when coupled with doped lanthanum gallate (LSGM) electrolyte (Dotelli et al., 2006). In this case the reduced electrochemical activity of LSM downgrades the cell performance and alternative cathode materials for IT-SOFCs are needed (Yi and Choi, 2004, Mai et al., 2005). One drawback of using porous LSM when operating below 800°C is the poor oxygen ion conduction, which limits the active area of the electrode to the three phase boundary (TPB) between electrolyte, electrode and gas phase at the interface. Moreover, it is known that manganese is a mobile species at high temperature; the occurrence of cations interdiffusion between LSM and LSGM both during the sintering step at elevated temperatures and at working temperatures for intermediate temperature SOFC has been reported (Pelosato et al., 2004). Thus to minimise manganese migration the fabrication temperature has to be kept below 1200°C. To overcome the limitations of traditional LSM, the use of doped- LaCoO_3 (LSCo) has been proposed (Skinner, 2001). However, Co and Fe diffusivities in LSGM and concomitant Mg and Ga diffusivities in LSFco were observed (Sakai et al., 2006). Moreover, the thermal expansion mismatch between LSFco cathode and LSGM electrolyte may lead to insufficient contact points and thus to the detachment of cathode layers, which limits the applications of cobalt containing cathode materials. Substituted $\text{La}_{1-x}\text{Sr}_x\text{FeO}_3$ (LSF) are promising cathodic materials. The Cu substituted LSF (LSFCu) series was first proposed as oxygen electrode in IT- SOFCs by Coffey et al. (2004), who reported that Cu doping improves both the electrocatalytic activity and the electrical conductivity compared with the parent LSF material. Recently, Mancini et al., (2014) reported that LSFCu might be a suitable cathode material for SOFC

operating below 800°C. The feasibility of LSF_{Cu} as cathode material for IT-SOFCs has been demonstrated on the basis of structural (Natali Sora et al., 2012), thermal and electrochemical studies (Vogt et al., 2009). The material has been tested with different electrolytes such as GDC (Coffey et al., 2004), YSZ (Yasumoto et al., 2002), and LSGM (Zurlo et al., 2014).

Cathodic materials specifically developed for SOFCs $\text{La}_{1-x}\text{Sr}_x\text{Fe}_{1-y}\text{Ta}_y\text{O}_{3-w}$ (LSFT) were prepared. Several physical properties of perovskite-type oxides are critically related to structural features (e.g. structural distortions from the ideal cubic perovskite structure). In LSF series three crystallographic regions are observed: orthorhombic symmetry for $0 \leq x \leq 0.2$, a mixture of both rhombohedral and orthorhombic phases for $x = 0.3$, rhombohedral for $0.4 \leq x \leq 0.7$ and cubic for $0.8 \leq x \leq 1.0$ (Dann et al., 1994). In this work we focus on the synthesis and characterization of LSFT, with and without Ta substitution on the B-site. In particular, we present the phase relations and structural properties of $\text{La}_{1-x}\text{Sr}_x\text{Fe}_{1-y}\text{Ta}_y\text{O}_3$ in the compositional range $x = 0 - 0.6$, $y = 0 - 0.15$. The phase relations and structural properties that occur in the LSFT series are compared with those of LSF_{Cu} series which has been investigated in detail by Natali Sora et al., (2012) using neutron diffraction data.

2. Experimental

2.1 Solid State Synthesis

$\text{La}_{1-x}\text{Sr}_x\text{Fe}_{1-y}\text{Ta}_y\text{O}_{3\pm w}$ (LSFT) powders with compositions $x = 0$ and $y = 0, 0.05, 0.10$; $x = 0.20$ and $y = 0, 0.05, 0.10$; $x = 0.30$ and $y = 0.05$; $x = 0.40$ and $y = 0, 0.05, 0.10, 0.15$; $x = 0.60$ and $y = 0, 0.05, 0.10, 0.15$ were prepared by solid state reaction. Dried La_2O_3 , SrCO_3 , Fe_2O_3 and Ta_2O_5 powders were mixed and ground together in an agate mortar for 30 min. All reagents were used in analytical grade and supplied by Sigma-Aldrich. The powder mixture was pressed into a pellet and thermal treated at 1000°C for 24 h and then at 1350°C for 24h, with an intermediate grinding step between the thermal treatments.

2.2 X-ray Diffraction

For each composition phase purity, lattice symmetry, and unit-cell parameters were determined by powder X-ray diffraction. The measurement was performed in Bragg-Brentano geometry, with 0.02° increment size and collection time of 1 sec/step over the 2-Theta angular range 5-70°. For more than 0.05 mol% of Ta several peaks belonging to secondary phases were detected in the diffraction patterns. For those compositions where no impurity peaks were present in the diffraction data, LaFeO_3 , $\text{LaFe}_{0.95}\text{Ta}_{0.05}\text{O}_3$, $\text{La}_{0.80}\text{Sr}_{0.20}\text{Fe}_3$, $\text{La}_{0.80}\text{Sr}_{0.20}\text{Fe}_{0.95}\text{Ta}_{0.05}\text{O}_3$, $\text{La}_{0.60}\text{Sr}_{0.40}\text{FeO}_3$, $\text{La}_{0.60}\text{Sr}_{0.40}\text{Fe}_{0.95}\text{Ta}_{0.05}\text{O}_3$, $\text{La}_{0.40}\text{Sr}_{0.60}\text{FeO}_3$, and $\text{La}_{0.40}\text{Sr}_{0.60}\text{Fe}_{0.95}\text{Ta}_{0.05}\text{O}_3$, the XRD patterns were collected a second time with longer counting time (10 s per step) in the 2θ range 5 - 90°. The structural refinements were carried out with the Rietveld method of profile analysis using GSAS (Larson and Von Dreele, 2000). The end-member phase LaFeO_3 was reported to have orthorhombic $\sqrt{2}a_p \times 2a_p \times \sqrt{2}a_p$ cell (where a_p denotes the unit-cell lattice parameters of the perovskite subcell). The first set of refinements was made assuming as structural model the perovskite-like cell of LaFeO_3 and the symmetry of space group *Pnma* (Caronna et al., 2009). The refined parameters included scale factor, background function (Chebyshev polynomial), profile parameters (pseudo-Voigt profile function), lattice parameters, atomic coordinates and isotropic temperature factors. Throughout the refinements, the fractional site occupancies of cations were fixed to the nominal values. Since laboratory powder X-ray diffraction data do not allow determining the accurate site occupancy of oxygen atoms due to the small value of the oxygen scattering factor, the fractional occupancy of the oxygen atoms remained unitary. During the refinements the atomic coordinates and the temperature factors of the La/Sr and Fe/Ta sites were constrained to be the same; the temperature factors for both crystallographic independent oxygen atoms, O(1) and O(2), were also forced to be the same.

3. Results and Discussion

3.1 XRD Analysis

In Figure 1 the XRD patterns of the $\text{LaFe}_{1-y}\text{Ta}_y\text{O}_3$ powders with $y = 0, 0.05$ and 0.10 are shown. $\text{LaFe}_{0.95}\text{Ta}_{0.05}\text{O}_3$ has the same basic structure of LaFeO_3 which crystallized with the orthorhombic symmetry (space group *Pnma*), and the refined cell parameters were $a = 5.56139(9)$ Å, $b = 7.85911(11)$ Å, $c = 5.55946(8)$ Å and $V = 242.990(6)$ Å³. For $y = 0.10$ molar content of Ta small amount of LaTaO_4 , and traces of Ta_2O_5 were present. The ideal ABO_3 perovskite structure has cubic symmetry and consists of a structural framework of corner-sharing BO_6 octahedra: the larger A cations are located in cuboctahedral sites, and the smaller B cations in octahedral sites.

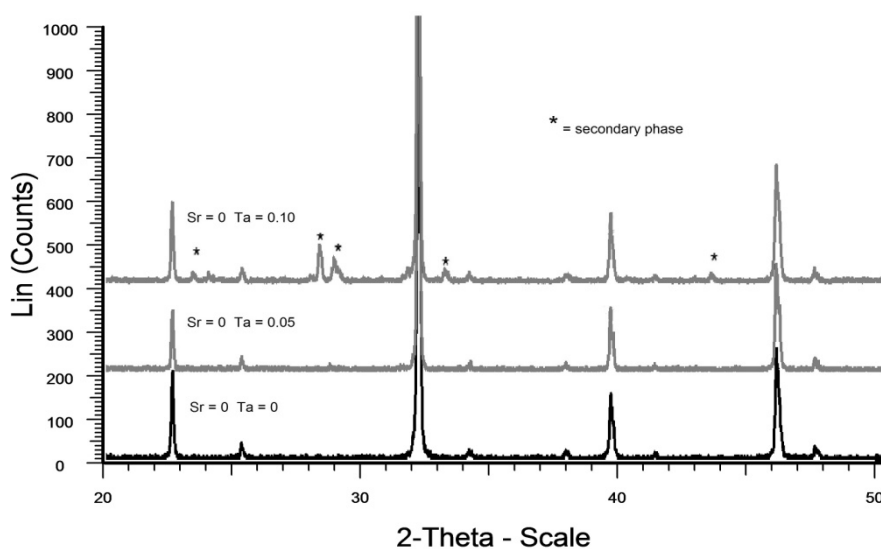


Figure 1: XRD patterns of $\text{LaFe}_{1-y}\text{Ta}_y\text{O}_3$ powders with $y = 0, 0.05$ and 0.10

Few ABO_3 compounds have this ideal cubic structure, many of them having slightly distorted variants with lower symmetry. The perovskite structure may accommodate cations of different ionic size in the unit cell, for example when Sr^{2+} is substituted for La^{3+} a solid solution with a wide miscibility range is obtained. In Figure 2 the orthorhombic crystal structure of $\text{La}_{0.80}\text{Sr}_{0.20}\text{Fe}_{0.95}\text{Ta}_{0.05}\text{O}_3$ is shown. The La atoms have twelve neighbouring oxygen atoms. The Fe and Ta atoms are randomly distributed over the positions 0,0,1/2 and have octahedral coordination. $\text{La}_{0.80}\text{Sr}_{0.20}\text{Fe}_{0.95}\text{Ta}_{0.05}\text{O}_3$ crystallized in the orthorhombic symmetry space group $Pnma$, and refined cell parameters were $a = 5.56068(11) \text{ \AA}$, $b = 7.84470(15) \text{ \AA}$, $c = 5.54733(12) \text{ \AA}$ and $V = 241.985(8) \text{ \AA}^3$. For $y = 0.10$ molar content of Ta small amount of $\text{Sr}_2\text{FeTaO}_6$ was present. For $\text{Sr} = 0.30$ the presence of a mixture of both rhombohedral and orthorhombic phases and a certain low quality of the data suggested to omit the refinement. In Figure 3 the XRD patterns of the $\text{La}_{0.60}\text{Sr}_{0.40}\text{Fe}_{1-y}\text{Ta}_y\text{O}_3$ powders with $y = 0, 0.05, 0.10$ and 0.15 are shown. It was observed (see the magnification of the 2-theta range $31.4^\circ - 35.9^\circ$) that the crystal symmetry of the main perovskite phase varied with increasing Ta molar content. For $\text{La}_{0.60}\text{Sr}_{0.40}\text{Fe}_{0.95}\text{Ta}_{0.05}\text{O}_3$ the Rietveld refinements gave much better results using the rhombohedral structural

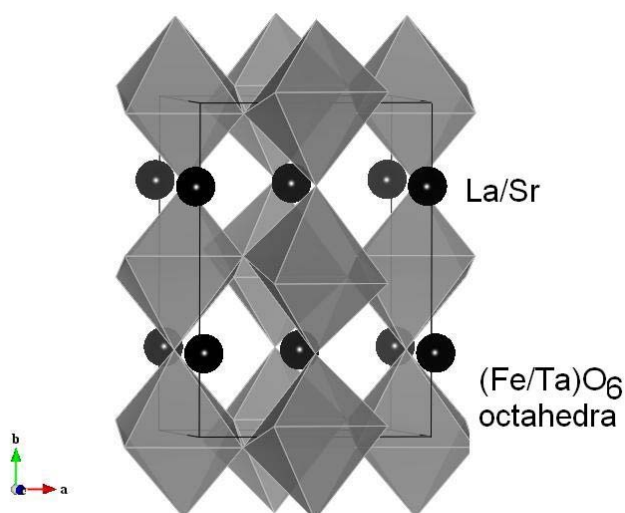


Figure 2: Orthorhombic crystal structure of $\text{La}_{0.80}\text{Sr}_{0.20}\text{Fe}_{0.95}\text{Ta}_{0.05}\text{O}_3$ showing the $(\text{Fe}/\text{Ta})\text{O}_6$ octahedra, large circles represent La/Sr cations

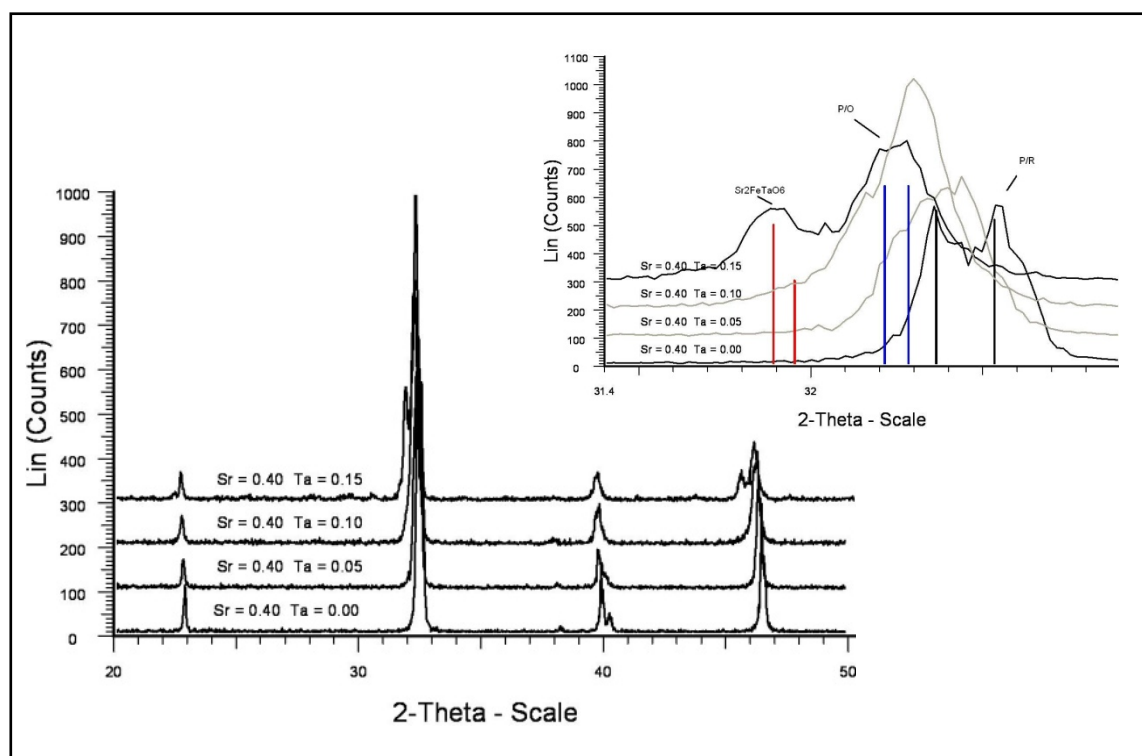


Figure 3: XRD patterns of $\text{La}_{0.60}\text{Sr}_{0.40}\text{Fe}_{1-y}\text{Ta}_y\text{O}_3$ powders with $y = 0, 0.05, 0.10$ and 0.15 . In the enlargement P/O indicates the orthorhombic perovskite phase, P/R indicates the rhombohedral perovskite phase

model of $\text{La}_{0.60}\text{Sr}_{0.40}\text{FeO}_3$, which crystallizes with the rhombohedral symmetry (space group $R\bar{3}c$). The refined cell parameters of $\text{La}_{0.60}\text{Sr}_{0.40}\text{Fe}_{0.95}\text{Ta}_{0.05}\text{O}_3$ were $a = 5.54322(7)$ Å, $c = 13.4719(3)$ Å and $V = 358.50(1)$ Å³. For $\text{Ta} = 0.10$ molar content a mixture of orthorhombic perovskite (P/O), rhombohedral perovskite (P/R) and small amount of $\text{Sr}_2\text{FeTaO}_6$ were present. For $\text{Ta} = 0.15$ two phases, a main orthorhombic perovskite (P/O) and small amount of $\text{Sr}_2\text{FeTaO}_6$, were identified. $\text{La}_{0.40}\text{Sr}_{0.60}\text{Fe}_{1-y}\text{Ta}_y\text{O}_{3-w}$ powders with $y = 0, 0.05, 0.10$ and 0.15 also were studied. For $\text{Ta} = 0.05$ a single rhombohedral perovskite was detected, on the contrary for $\text{Ta} = 0.10$ and 0.15 molar content the compounds were biphasic; the mixture consisted in a main rhombohedral perovskite (P/R) and small amount of $\text{Sr}_2\text{FeTaO}_6$.

In order to compare how the Sr and Ta substitution influenced the structure of the perovskite, the pseudocubic unit cell volume V_c was calculated as $V_c = V / Z$, where $Z = 4$ for the orthorhombic perovskite, and $Z = 6$ for the rhombohedral perovskite. For $\text{Ta} = 0.05$ V_c decreased with increasing Sr molar content, in accordance with

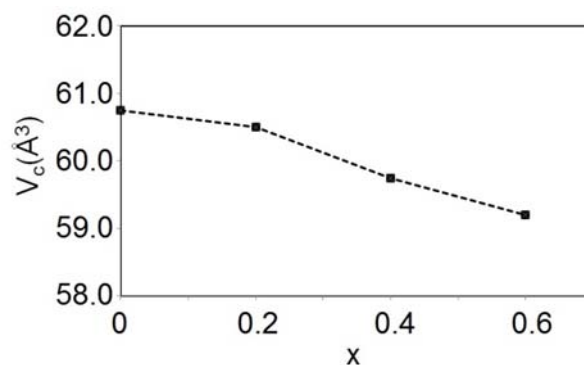


Figure 4: the pseudo-cubic unit cell volume ($V_c = V / Z$) for the series $\text{La}_{1-x}\text{Sr}_x\text{Fe}_{0.95}\text{Ta}_{0.05}\text{O}_3$ as a function of the Sr content

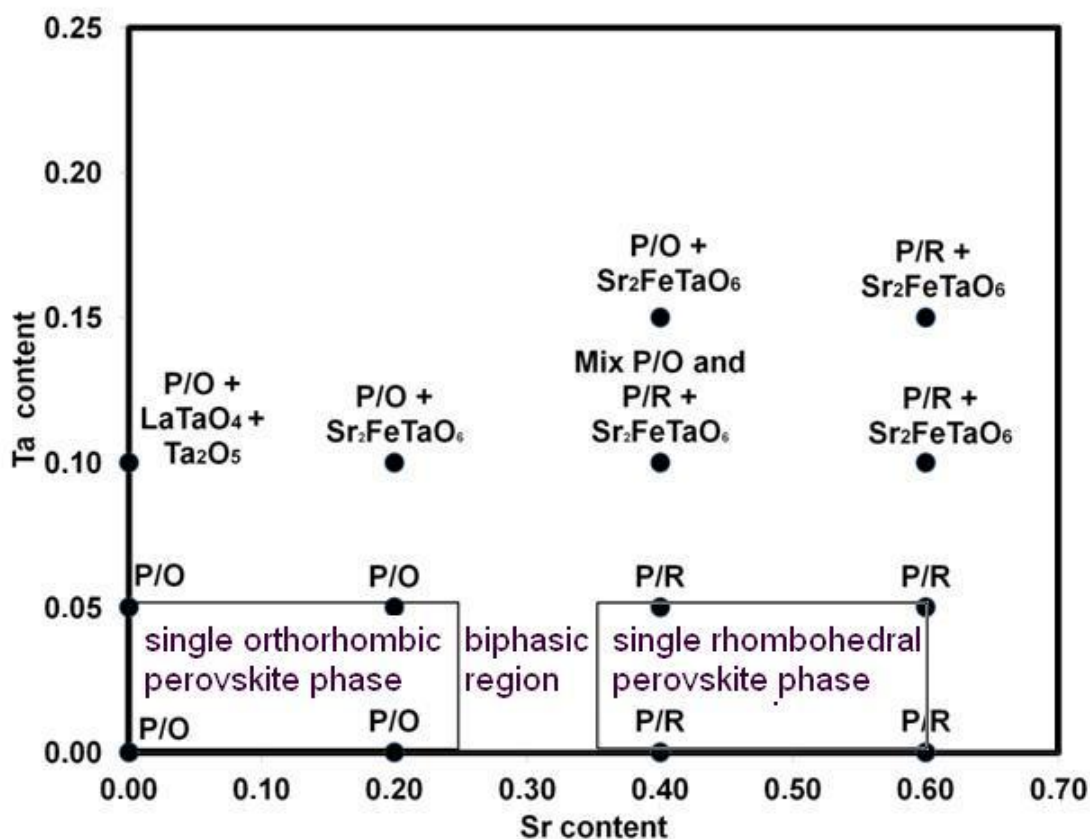


Figure 5: phase compositions of the series $La_{1-x}Sr_xFe_{1-y}Ta_yO_{3±w}$ studied in this work are summarized. P/O indicates the orthorhombic perovskite phase, P/R indicates the rhombohedral perovskite phase

the trend known for $La_{1-x}Sr_xFeO_{3-w}$ where $V_c^{orth} > V_c^{rhomb}$ (Figure 4).

Moreover, when Sr was kept constant V_c increased with increasing Ta molar content. For example the values of V_c were 59.75 Å and 60.29 Å for $La_{0.60}Sr_{0.40}Fe_{0.95}Ta_{0.05}O_3$ and $La_{0.60}Sr_{0.40}Fe_{0.90}Ta_{0.10}O_3$. To maintain the charge balance, Ta^{5+} and Fe^{3+} cations may be in a valence state smaller than +5 and +3, respectively. The values of the ionic radius are: $Ta^{5+}(VI) = 0.64$ Å and $Ta^{4+}(VI) = 0.66$ Å, and $Fe^{3+}(VI) = 0.645$ Å and $Fe^{2+}(VI) = 0.77$ Å (Shannon and Prewitt, 1969). Since the reduced cations are larger, they are under compressive stress. The lattice strain introduced in the structure may cause phase demixing. In Figure 5 are summarized the phase relationships and the structural properties of the system $La_{1-x}Sr_xFe_{1-y}Ta_yO_{3±w}$ studied in this work. The single phase regions of LSFT are much smaller with respect to the Ta content in comparison with those of the LSFCu series varying Cu. In particular, for $x = 0.20$ and Cu content in the range 0 - 0.10 LSFCu crystallizes in an orthorhombic phase with space group $Pnma$ (Natali Sora et al., 2013), while for $x = 0.20$ and $y = 0.20$ the powders are a mixture of both orthorhombic and rhombohedral perovskite phases (Natali Sora et al., 2012). The investigation on the electrochemical behaviour of LSFT-based cathodes is ongoing.

4. Conclusions

A series of compounds of the $La_{1-x}Sr_xFe_{1-y}Ta_yO_3$ system of interest as cathodic catalysts in SOFCs have been prepared using solid state reaction method. Three crystallographic regions were observed by X-rays diffraction studies for $Ta \leq 0.05$: orthorhombic symmetry for $0 \leq x \leq 0.2$, a mixture of both rhombohedral and orthorhombic phases for $x = 0.3$, rhombohedral symmetry for $0.4 \leq x \leq 0.6$. In particular, $LaFeO_3$, $LaFe_{0.95}Ta_{0.05}O_3$, $La_{0.80}Sr_{0.20}Fe_3$, and $La_{0.80}Sr_{0.20}Fe_{0.95}Ta_{0.05}O_3$ crystallized in the orthorhombic perovskite structure (space group $Pnma$). $La_{0.60}Sr_{0.40}Fe_3$, $La_{0.60}Sr_{0.40}Fe_{0.95}Ta_{0.05}O_3$, $La_{0.40}Sr_{0.60}FeO_3$, and $La_{0.40}Sr_{0.60}Fe_{0.95}Ta_{0.05}O_3$, crystallized in the rhombohedral perovskite structure (space group $R-3c$). When the Ta molar content was $0.05 < y \leq 0.10$, and the Sr molar content was $0 \leq x \leq 0.20$, the samples showed a secondary phase. For $x = 0$ the main impurity was $LaTaO_4$, while for $x = 0.20$ Sr_2FeTaO_6 was found as

secondary phase. For higher Sr substitution ($0.40 \leq x \leq 0.60$) a larger Ta compositional region was investigated $0.05 < y \leq 0.15$; in this area all samples showed a secondary phase $\text{Sr}_2\text{FeTaO}_6$.

Acknowledgements

The financial support and collaboration of INSTM and of the Lombardy Region (Project "Ferriti di lantanio per nuove Fonti di Energia", Ferriti-NFE) 2013-2015 is gratefully acknowledged. The financial support of Università di Bergamo (ITALY® (Italian TALEnted Young @esearchers) - Project Corrosion Models in Presence of Scale, CoSca) 2013-2014.

References

- Caronna T., Fontana F., Natali Sora I., Pelosato R., 2009, Chemical synthesis and structural characterization of the substitution compound $\text{LaFe}_{1-x}\text{Cu}_x\text{O}_3$ ($x = 0-0.40$), *Mat. Chem. Phys.* 116, 645-648
- Coffey G., Hardy J., Marina O., Pederson L., Rieke P., Thomsen E., 2004, Copper doped lanthanum strontium ferrite for reduced temperature solid oxide fuel cells, *Solid State Ionics* 175, 73-78
- Dann S.E., Currie D.B., Weller M.T., Thomas M.F., Al-Rawwas A.D., 1994, The Effect of Oxygen Stoichiometry on Phase Relations and Structure in the System $\text{La}_{1-x}\text{Sr}_x\text{FeO}_{3-\delta}$ ($0 \leq x \leq 1$, $0 \leq \delta \leq 0.5$) *Solid State Chem.* 109, 134-144
- Dotelli G., Mari C. M., Ruffo R., Pelosato R., Natali Sora I., 2006, Electrical behaviour of LSGM-LSM composite cathode materials, *Solid State Ionics* 177, 1991-1996
- Larson A. C. and Von Dreele R. B., 2000, General Structure Analysis System (GSAS) program, Los Alamos National Laboratory Report LA-UR-86-748.
- Mai A., Haanappel V.A.C., Uhlenbruck S., Tietz F., Stöver D., 2005, Ferrite-based perovskites as cathode materials for anode-supported solid oxide fuel cells. Part I. Variation of composition, *Solid State Ionics* 176, 1341-1350
- Mancini A., Felice V., Natali Sora I., Malavasi L., Tealdi C., 2014, Chemical compatibility study of melilite-type gallate solid electrolyte with different cathode materials, *J. Solid State Chem.* 213, 287-292
- Natali Sora I., Caronna T., Fontana F., De Julián Fernández C., Caneschi A., Green M., 2012, Structural and Magnetic Properties of $\text{La}_{0.8}\text{Sr}_{0.2}\text{Fe}_{1-x}\text{Cu}_x\text{O}_{3-w}$ ($x = 0.05, 0.10$ and 0.20), *J. Solid State Chem.* 191, 33-39
- Natali Sora I., Fontana F., Passalacqua R., Ampelli C., Perathoner S., Centi G., Parrino F., Palmisano L., 2013, Photoelectrochemical properties of doped lanthanum orthoferrites, *Electrochimica Acta* 109, 710-715
- Pelosato R., Natali Sora I., Ferrari V., Dotelli G., Mari C.M., 2004, Preparation and characterization of supported $\text{La}_{0.83}\text{Sr}_{0.17}\text{Ga}_{0.83}\text{Mg}_{0.17}\text{O}_{2.83}$ (LSGM) thick films for application in IT-SOFCs, *Solid State Ionics* 175, 87-92
- Sakai N., Horita T., Yamaji K., Brito M.E., Yokokawa H., Kawakami A., Matsuoka S., Watanabe N., Ueno A., 2006, Interface Stability among Solid Oxide Fuel Cell Materials with Perovskite Structures, *J. Electrochem. Soc.* 15, A621-A625
- Shannon R.D., Prewitt C.T., 1969, Effective Ionic Radii in Oxides and Fluorides, *Acta Crystallographica B* 25, 925-946
- Skinner, S. J., 2001, Recent advances in perovskite-type materials for solid oxide fuel cell cathodes, *Int. Journal. Inorg. Mater.* 3, 113
- Vogt U.F., Holtappels P., Sfeir J., Richter J., Duval S., Wiedenmann D, Zütten A., 2009, Influence of A-Site Variation and B-Site Substitution on the Physical Properties of (La,Sr)FeO₃ Based Perovskites, *Fuel Cells* 9, 899-906
- Yasumoto K., Inagaki Y., Shiono M., Dokiya M., 2002, An (La,Sr)(Co,Cu)O_{3-δ} cathode for reduced temperature SOFCs, *Solid State Ionics* 148, 545-549
- Yi J.Y., Choi G.M., 2004, Cathodic properties of $\text{La}_{0.9}\text{Sr}_{0.1}\text{MnO}_3$ electrode for fuel cells based on LaGaO_3 solid electrolyte, *J. Eur. Ceram. Soc.* 24, 1359-1363
- Zurlo F., Di Bartolomeo E., D'Epifanio A., Felice V., Natali Sora I., Tortora L., Licocchia S., 2014, $\text{La}_{0.8}\text{Sr}_{0.2}\text{Fe}_{0.8}\text{Cu}_{0.2}\text{O}_{3-\delta}$ as "cobalt free" cathode for $\text{La}_{0.8}\text{Sr}_{0.2}\text{Ga}_{0.8}\text{Mg}_{0.2}\text{O}_{3-\delta}$ electrolyte, *J. Power Sources* 271, 187-194